Solid State Sciences 68 (2017) 1–9

Contents lists available at ScienceDirect

Solid State Sciences

journal homepage: www.elsevier.com/locate/ssscie

Solid state synthesis, spectroscopic and X-ray studies of metal complexes of 2-picolinic acid and vapochromic behavior of $[Co(Pic)_2(H_2O)_2]\cdot 2H_2O$

Adedibu C. Tella [a, *], Adetola C. Oladipo [a], Olalere G. Adeyemi [b], Oluwatobi S. Oluwafemi [c, d, **], Stephen O. Oguntoye [a], Lukman O. Alimi [e], Joseph T. Ajayi [f], Sylvestre K. Degni [a]

[a] Department of Chemistry, P.M.B.1515, University of Ilorin, Nigeria
[b] Department of Chemical Sciences, Redeemer's University, Ede, Nigeria
[c] Department of Applied Chemistry, University of Johannesburg, P.O. Box 17011, Doornfontein, Johannesburg 2028, South Africa
[d] Centre for Nanomaterials Science Research, University of Johannesburg, Johannesburg, South Africa
[e] Department of Chemistry and Polymer Science, Stellenbosch University, Stellenbosch 7602, South Africa
[f] Organometallic Synthetic Laboratory, School of Chemistry and Physics, University of KwaZulu Natal, Durban, South Africa

ARTICLE INFO

Article history:
Received 7 November 2016
Received in revised form
26 February 2017
Accepted 11 March 2017
Available online 4 April 2017

Keywords:
Solvent-free synthesis
PXRD
2-Picolinic acid
Vapochromism
Simulated pattern

ABSTRACT

Three compounds, $[Cu(Pic)_2(H_2O)]$ **(1a),** $[M(Pic)_2(H_2O)_2]\cdot 2H_2O$ (M=Co **(2a),** Zn **(3a)**, Pic = 2-picolinic acid) were obtained by solvent-free synthesis through grinding of metal acetate salt with 2-picolinic acid. Favorable comparison of solvent-free with solution based method of 1b, 2b and 3b was observed. Good resemblance of identity of compounds obtained through the two methods was confirmed by elemental analysis, spectroscopic techniques (UV-Vis and FTIR), TGA and PXRD. The single crystal diffraction data for $[Co(Pic)_2(H_2O)_2]\cdot 2H_2O$ obtained from the Cambridge structure database (CSD), its PXRD simulated patterns closely matched that of complex **2a** by solvent-free synthesis. Vapochromic behavior of this complex was studied using colour change, FT-IR, TGA, PXRD and solid state UV-visible spectroscopies. This complex generated specific colour which is also evident in the shifting of the vibrational frequencies (νO-H and ν C=O bands). The resulting inclusion compounds have different colours depending on the solvent used. In addition, exposure of the resultant inclusion compounds to ambient environment or heating for a few minutes regenerate the original material without degradation even after exposure/heating cycles as evident from TGA/DTG thermograms.

© 2017 Elsevier Masson SAS. All rights reserved.

1. Introduction

2-picolinic acid (PA) is a six-membered ring structure and an isomer of nicotinic acid, containing five carbon atoms, a nitrogen and a carboxyl group at position 2. 2-picolinic acid is an endogenous metabolite of L-tryptophan (TRP) that has been reported to possess a wide range of medicinal values [1]. A good number of 2-picolinic acid and its metal complexes synthesized using solvent-based synthesis have been reported to possess a wide range of neuroprotective, immunological, therapeutic and anti-proliferative effects within the body [2–6]. The picolinate ion structure has two carboxylate oxygen atoms and one pyridyl nitrogen atom as potential donor sites leading to a variety of ligation modes [1]. In recent years, solvent-less chemistry has gained much attention in both academic and industrial laboratories. For instance, one of the major targets in green chemistry is to limit the extensive use of solvents or even better solvent less reaction. Solvent free or solvent less reactions (system in which neat reagents react together, in the absence of a solvent) are thought to occur in the solid phase. Many coordination complexes have been readily formed by grinding simple transition metal starting materials with potential ligands [7–9]. Also, mechanochemical synthesis of drug-metal complexes [10–14] and metal organic frameworks by manual grinding with

* Corresponding author. Department of Chemistry, P.M.B.1515, University of Ilorin, Nigeria.
** Corresponding author. Department of Applied Chemistry, University of Johannesburg, P.O. Box 17011, Doornfontein, Johannesburg 2028, South Africa.
E-mail addresses: ac_tella@yahoo.co.uk (A.C. Tella), oluwafemi.oluwatobi@gmail.com (O.S. Oluwafemi).

http://dx.doi.org/10.1016/j.solidstatesciences.2017.03.017
1293-2558/© 2017 Elsevier Masson SAS. All rights reserved.

mortar and pestle or by ball-milling have also been reported [15–20].

When two solids are grounded together, the heat generated in the grinding process may be sufficient to induce local melting of the solid reagents. This lead to generation of a hot spot(exothermic) during initial grinding of the solids resulting in the formation of a liquid melt phase [21,22]. However, it was generally observed that, the reaction proceeded via intermediate eutectic liquid melt phase before product formation [23].

Vapochromic materials, which display colour (optical absorption) or luminescence changes upon exposure to vapours of volatile organic compounds (VOCs), are of great interest due to their potential applications for chemical vapour detection [8,24–32].

To the best of our knowledge, none of the 2-picolinic -metal complexes have been synthesized using the solid-state reaction, thus, we applied solid-state reaction to synthesize metal complexes of picolinic acid. In addition, the cobalt (II) picolinic complex was tested against solvent vapours. The complex displayed colour change, which positioned it as a vapochromic sensor.

2. Experimental

All reagents and chemicals were obtained from commercial sources and were of analytical grade. The melting points of the complexes were determined using a Gallen-Kamp melting point apparatus. FT-IR Spectra of the ligand and the complexes were recorded in KBr pellets in the range of 4000–400 cm^{-1} on a SHIMADZU scientific model 500 FITR spectrophotometer. Electronic spectra were done using SHIMADZU UV-1650pc UV-VIS spectrophotometer. Elemental analyses were performed on a Perkin-Elmer CHN Analyzer 2400 Series II. Powder XRD analysis was performed on a syntax PADS diffractometer at 294K using CuKα radiation (λ = 1,54059 Å). Thermogravimetric analyses (TGA) were recorded with a TA instrument (TA-Q500). The sample weight was approximately1–2 mg and a heating rate of 10 °C min^{-1} under a nitrogen gas flow of 50 mL min^{-1} was used.

2.1. General synthetic procedure

The methods described by Silva *et al* [33] were modified for the solvent-based synthesis while the method described by Pichon *et al* [20] was modified for the mechanochemical synthesis.

2.2. Mechanochemical solvent-free synthesis of (1a -3a)

A typical synthetic route is described for **1a.** 2-picolinic acid (0.246 g, 2 mmol) and [$Cu(CH_3COO)_2 \cdot H_2O$] (0.199 g, 1 mmol) were accurately weighed into an agate mortar which had been washed and dried. The reactants were ground together continuously for 15 min. The blue powder obtained was washed with methanol to remove unreacted starting materials and dried at room temperature. The chemical equation of the reaction is shown in Scheme 1.

1a. Yield: 75%, M.wt. = 328 g/mol, M.pt. >300 °C Anal. Found (Calcd) % for ($C_{12}H_{10}N_2O_5Cu$): C, 44.03 (44.17); H, 3.13 (3.07); N, 8.64 (8.59), IR (KBr, cm^{-1}): 3439, 3271, 2360, 1715, 1641, 1570, 1356, 694, 559, 455; UV-Vis (DMSO) nm = 679; Powder X-ray diffraction (Cu-Kα) 2θ = 11.60, 13.23, 14.66, 19.54, 23.56, 24.78 and 28.10.

Compound **2a** was prepared by similar procedure for the synthesis of **1a** above except that cobalt acetate [$Co(CH_3COO)_2 \cdot 4H_2O$] (0.249 g, 1 mmol) was used instead of [Cu ($CH_3COO)_2 \cdot H_2O$].

Yield: 90%, M.wt. = 374 g/mol, M.pt. = 274 °C, Anal. Found (Calcd) % for ($C_{12}H_{16}N_2O_8Co$): C, 38.43 (38.50); H, 4.32 (4.26); N, 7.61 (7.47), IR (KBr, cm^{-1}): 3398, 3066, 2360,1713, 1626, 1568, 1373, 642, 570, 445; UV-Vis (DMSO) nm: 415, 475, 752; Powder X-ray diffraction (Cu-Kα) 2θ = 10.85, 12.19, 18.17,20.42, 22.42, 22.89, 25.68, 26.68, 27.85 and 31.37.

Compound **3a** was prepared by similar procedure for the synthesis of 1a above except that [Zn ($CH_3COO)_2 \cdot 2H_2O$ (0.220 g, 1 mmol) was used instead of [Cu ($CH_3COO)_2 \cdot H_2O$].

1. Yield: 87%, M.wt. = 381 g/mol, M.pt. = 257 °C, Anal. Found (Calcd) % for ($C_{12}H_{16}N_2O_8Zn$): C, 37.68 (37.80); H, 4.17 (4.20); N, 7.28 (7.35), IR (KBr,cm^{-1}): 3383, 2360, 1715, 1653, 1599, 1384, 1049, 881, 692, 573, 475; UV-Vis (DMSO) nm: 216, 288; Powder X-ray diffraction (Cu-Kα) 2θ = 8.38, 11.32, 12.86, 14.09, 15.54, 21.44, 23.60, 25.34, 26.56 and 31.33.

2.3. Solvent-based synthesis of (1b-3b)

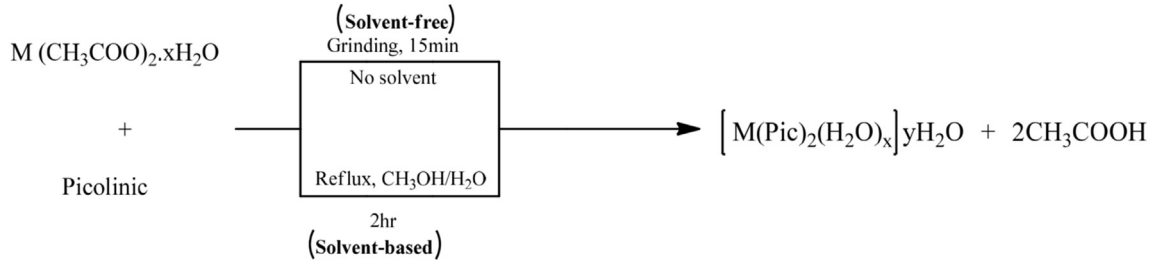
A typical synthetic route is described for 1b. 2-picolinic acid (0.246 g, 2 mmol) and copper acetate [Cu ($CH_3COO)_2$. H_2O] (0.199 g, 1 mmol) were dissolved in distilled water (10 mL) and stirred for 40 min, followed by the addition of methanol (5 mL). The mixture was refluxed for 2 h. A clear blue solution was obtained and left standing for slow evaporation at room temperature. Blue crystals were formed after 24 days, washed in methanol and dried at room temperature. The chemical equation of reaction is shown in Scheme 1.

Yield: 63%, M.wt. = 328 g/mol, M.pt. > 300 °C, Anal. Found (Calcd) % for ($C_{12}H_{10}N_2O_5Cu$): C, 44.19 (44.17); H, 3.03 (3.07); N, 8.45 (8.59), IR (KBr, cm^{-1}): 3439, 3064, 2522, 1714, 1614, 1570, 1356, 659, 569, 453; UV-Vis (DMSO) nm = 676; Powder X-ray diffraction (Cu-Kα) 2θ = 11.74,13.02, 15.02, 19.54, 23.55, 25.00 and 28.97.

Compound **2b** was prepared by a procedure similar to the synthesis of **1b** above except that cobalt acetate [$Co(CH_3COO)_2 \cdot 4H_2O$] (0.249 g, 1 mmol) was used instead of [Cu ($CH_3COO)_2$. H_2O] and orange crystal was obtained after 50 days.

Yield: 78%, M.wt. = 374 g/mol, M.pt. = 280 °C, Anal. Found (Calcd) % for ($C_{12}H_{16}N_2O_8Co$): C, 38.44 (38.50); H, 4.25 (4.26); N, 7.46 (7.47), IR (KBr, cm^{-1}): 3356, 3066, 2360, 1714, 1627, 1568, 1373, 642, 571, 447; UV-Vis (DMSO) nm: 418, 474, 746. Powder X-ray diffraction (Cu-Kα) 2θ = 10.71, 11.99, 17.98, 20. 26, 21.60, 22.76, 25.48, 26.56, 28.17, 31.17, 32.30 and 38.50.

Compound **3b** was prepared by a procedure similar to the synthesis of **1b** above except that [$Zn(CH_3COO)_2 \cdot 2H_2O$ (0.220 g,



Scheme 1. General synthetic route of the metal complexes of Picolinic acid.

1 mmol) was used instead of [$Cu(CH_3COO)_2$. H_2O] and White crystal was obtained after 15 days.

Yield: 61%, M.wt. = 381 g/mol, M.pt. = 260 °C, Anal. Found (Calcd) % for ($C_{12}H_{16}N_2O_8Zn$): C, 37.75 (37.80); H, 4.24(4.20); N, 7.38 (7.35), IR (KBr, cm^{-1}): 3421, 2360, 1732, 1650, 1599, 1384, 883, 761, 694, 570, 478; UV-Vis (DMSO) nm: 264, 295. Powder X-ray diffraction (Cu-Kα) $2\theta = 8.36, 10.98, 12.84, 14.08, 15.54, 16.20, 18.90, 21.44, 23.60, 25.34, 26.54$ and 31.35.

2.4. Vapochromic studies

The procedure used by Jobbagy *et al* [34] was used for the solvatochromic studies of the complex **2a**. The synthesized complex **2a** after being activated by heating at 180 °C for 20 min to form **2d** was placed in small open containers. The containers were then placed in a larger vial containing each of the volatile oxygen, nitrogen donor solvent (methanol, ethanol, dimethyl formamide, dimethyl sulfoxide, dichloromethane, benzene and NH_4OH). The larger containers were then tightly closed for 24 h at room temperature. Change in colour was observed and vapochromic properties were monitored by taking FT-IR, TGA, PXRD and solid state UV-visible spectra before and after exposure.

3. Results and discussions

The solid state complexes **1a**, **2a** and **3a** were synthesized by manual grinding of the ligand and corresponding metal salts for 15 min and powder products were obtained. Using solvent-based method, blue crystals of complex **1b** were formed after 24 days, orange crystals of complex **2b** were formed after 50 days and colourless microcrystalline powder of complex **3b** was formed after 15 days. The physical and analytical data of the complexes are presented in Table S1.The complexes are stable in air. The yields obtained for **1a**, **2a** and **3a** ranges between 75 and 90% for solvent-free as compared to solvent-based products with yield in the range between 61 and 78%. The yields of mechanochemically synthesized products are higher than that of solvent-based products and the reaction time was short (15 min) with quantitative yield. No obvious peak of impurities or starting materials were detected as evidenced from close agreement between the PXRD simulated patterns of the single crystal diffraction data and that of products. It was also observed that the grinding of the reactants to achieve product occurred via an intermediate liquid melt phase as shown in Fig. 1.

The UV-visible, FTIR spectra and CHN clearly shows the formation of 1:2 metals to ligand compound, in agreement with the previous work by Agwara *et al* [35] Compounds from both methods of synthesis gave similar spectra data which are both different from that of the ligand. All the complexes have higher melting points and different colour from those of the ligand. The elemental analysis for C, H, N were also consistent with the formula units of the products. The complexes were insoluble in methanol but soluble in solvents having pronounced donor properties e.g. DMSO and DMF.

3.1. Infra-red spectra

Fig. 2, Figures S1 and S2 show comparison of the FT-IR spectra of the free ligand and, Cu(II), Co(II) and Zn(II) complexes respectively that was obtained via solvent-free mechanochemical and solvent-based methods.

It can be seen from Fig. 2, Figures S1 and S2 that, FT-IR spectra of the complexes synthesized by both methods are identical but different from that of the ligand. The relevant IR and frequencies of the ligand and the complexes are presented in Table S2. The IR spectroscopy data of 2-picolinic acid and its complexes confirm the coordination of the 2-picolinate ligand to the metals through the carboxylate oxygen and the pyridine N atom of the ligand. The IR spectra of all complexes show similar features. The absorption band in the range 3439–3356 cm^{-1} in the spectra of these complexes is due to ν(OH) vibrations originating from both lattice and coordinated water molecules. The broadness of the bands is attributed to the presence of strong hydrogen bonding in the complexes. The FT-IR spectra of the 2-picolinic acid contain broad absorption band at 2607-2152 cm^{-1} attributed to the existence of O-H-N type of intermolecular hydrogen bonding. The disappearance of this band in the complex confirmed that coordination is through the nitrogen atom and carboxylate oxygen [36]. The absorption bands of the asymmetric $\nu_{as}(COO^-)$ appears at 1641 cm^{-1}, 1626 cm^{-1} and ~1653 cm^{-1} respectively for the Cu(II),Co(II) and Zn(II) complexes obtained from both synthetic methods. Absorption bands of the symmetric $\nu_s(COO^-)$ also appears at 1356 cm^{-1}, 1373 cm^{-1} and 1384 cm^{-1} for the complexes respectively. The magnitude of separation ($\Delta\nu$) between [$\nu_{as}(COO^-)$ - $\nu_{as}(COO^-)$] determines the mode of coordination [37]. The ($\Delta\nu$) for the complexes are 285 cm^{-1} for Cu (II) complex, 253 cm^{-1} for Co (II) complex and 269 cm^{-1} for Zn (II) complex. This suggests unidentate coordination of the carboxylate group [38,39]. The 1595 cm^{-1} band of the ligand corresponding to ν(C=N) also shifted to 1570 cm^{-1} for the Cu (II) complexes, 1568 cm^{-1} for Co(II) complexes and 1599 cm^{-1} for the Zn(II) complexes. These features are quite suggestive of the coordination of ligand with the metals through nitrogen atom of pyridine ring. Bands around 570 - 569 cm^{-1} and 445 - 495 cm^{-1} corresponding to metal-nitrogen and metal-oxygen bonds were observed in the spectra of all the complexes, confirming the coordination through the oxygen of the carboxylic group and nitrogen of the pyridine ring. M-OH_2 peaks around 642 - 692 cm^{-1} of the complexes also confirm the presence of water in the system. Agwara *et al* [35] in their works also observed the presence of lattice and coordinated water molecules in the cobalt and zinc picolinic complexes and only coordinated water molecule in its copper complex.

3.2. Electronic spectra

The UV-Visible spectra of 2-picolinic acid and its complexes obtained from both solvent-based and mechanochemical methods as shown in Table S3 shows that the complexes obtained from both methods are identical, but at variant with that of the free picolinic

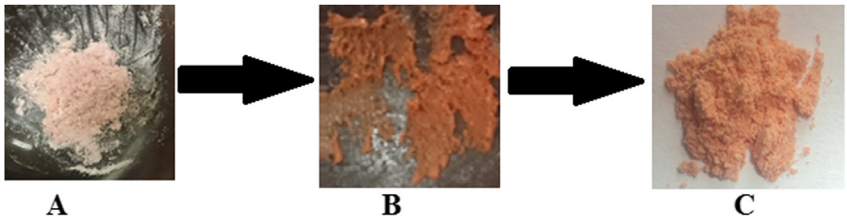


Fig. 1. Photographs of complex **2a** few minutes of grinding (**A**), intermediate melt-phase (**B**), and product (complex **2a**) (C).

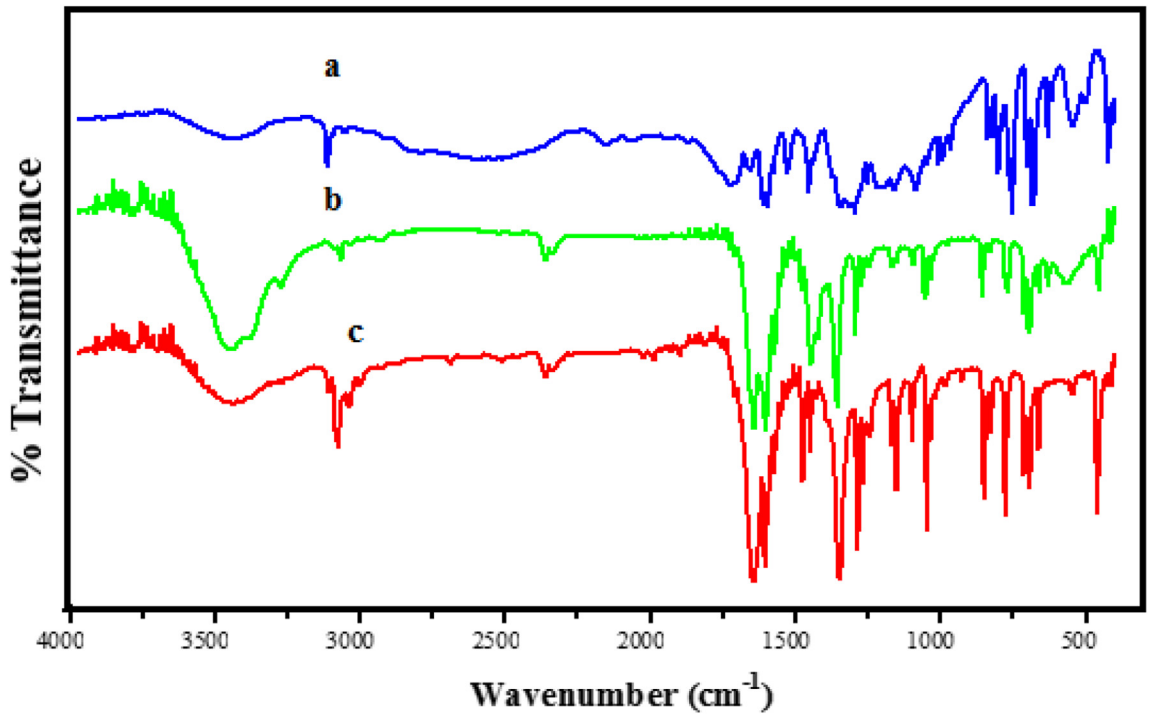


Fig. 2. FT-IR spectra of (a) 2-Picolinic acid (b) $Cu(Pic)_2(H_2O)$ (solvent-free) **1a** (c) $Cu(Pic)_2(H_2O)$ (solvent-based) **1b.**

acid. Table S3 shows that the UV-Vis spectrum of 2-picolinic acid has bands at 265 nm and 305 nm which are assigned to π-π^* and n-π^* respectively. In the visible spectrum of the copper complexes, the broad band was observed at ~676 nm assigned to the $^2Eg \rightarrow {}^2Tg$ transition [5]. The solvent-based and mechanochemical Co(II) complexes of 2-picolinic acid show three bands attributed to $^4T_{1g}$ - $^4T_{1g}(P)$, $^4T_{1g}$ - $^4A_{2g}$ and $^4T_{1g}$ - $^4T_{2g}$. suggesting an octahedral structure for the complexes. The spectra of the zinc complexes show no other bands other than those of the π-π^* and n-π^* transitions of the ligand.

3.3. X-ray diffraction studies

Comparison of the PXRD patterns (Fig. S3) during grinding process showed that, the reaction mixture initially in a solid state melted during the grinding leading to amorphous material as intermediate. Continuous grinding after 15 min produced product with patterns identical to simulated patterns obtained from x-ray single crystal data. This is in agreement with photographs (Fig. 1) taken during grinding process indicating that the reaction occurred via liquid melt phase. Figs. 3 and 4 and Fig. S4 show comparison of the X-ray diffraction patterns of the products **1**–**3** obtained via the solvent-based and solvent-free methods and the starting material. It can be observed that PXRD patterns of the products from solvent based and solvent-free techniques were identical and with almost equal positions of 2θ and intensities, but at variant with starting material, suggesting a formation of new metal complexes.

The PXRD pattern of the product **1a** revealed major peaks at 2θ = 11.60, 13.23, 14.66, 18.66,19.54, 23.56, 24.78 and 28.10 while those of simulated pattern (CSD letter code **YAVGAF**) were found to be at 11.34, 13.02, 14.74, 19.54, 24.16 and 28.67 (Fig. 3). For product **2a**, the PXRD of the major peaks at 2θ values are 10.85, 12.19, 18.17,20.42, 22.42, 22.89, 25.68, 26.68, 27.85 and 31.37 while its simulated patterns reported by Heren *et al* [40] (CSD code **APPICCO**) are at 11.00, 11.96,, 17.76, 19.32, 20.30, 22.52, 25.58, 26.66,

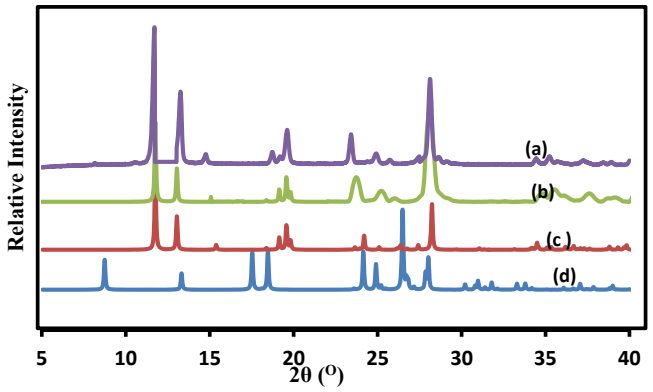


Fig. 3. Comparison of PXRD patterns of (a) $[Cu(Pic)_2(H_2O)]$**1a** (Solvent free) (b) $[Cu(pic)_2(H_2O)]$ **1b** (Solvent-based) (c) simulated patterns from x-ray single crystal (**YAVGAF**) and (d) 2-picolinic acid.

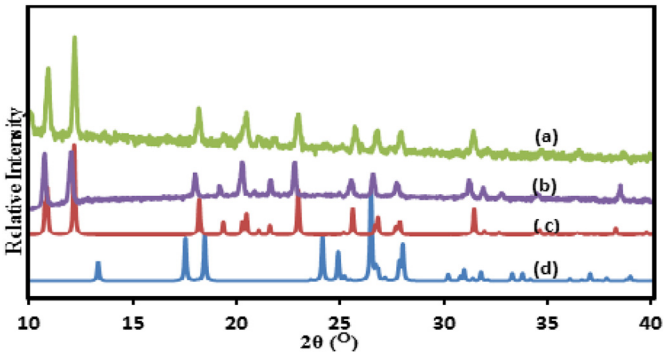


Fig. 4. Comparison of PXRD pattern of (a) $[Co(Pic)_2(H_2O_2)]2H_2O$ **2a** (Solvent-free) and (b) $[Co(Pic)_2(H_2O_2)]2H_2O$ **(2b)** (Solvent based (c) Simulated patterns from X-ray single crystal data (APPICCO) (d) 2-Picolinic acid.

27.68 and 31.44 (Fig. 4). The PXRD patterns major peaks present in **3** are 8.38, 11.32, 12.86, 14.09, 15.54, 21.44, 23.60, 25.34, 26.56 and 31.33; its simulated patterns(CSD code AGABER) were found at 8.36, 11.13, 12.88, 14.08, 15.54, 16.22, 18.90, 21.46, 23.62, 25.34, 26.58, 28.38 and 31.36 (Fig. S4). For the three complexes the simulated patterns of the single crystal diffraction data for $[Cu(pic)_2(H_2O)]$, $[Co(pic)_2(H_2O)_2]2H_2O$ and $Zn(pic)_2(H_2O)_2]2H_2O$ using mercury 1.3 software obtained from the Cambridge structural Database (CSD) and complexes **1a**, **2a** and **3a** obtained from mechanochemical synthesis were in close agreement. This justify the proposed structure along with other characterization techniques.

3.4. Thermal decomposition studies of the as-synthesized complex 2a

The thermogravimetric analysis curve of the complex **2a** is given in (Fig. 5). The thermal behavior of the complex was followed up to 600 °C. In the first stage of thermal decomposition, the complex shows weight loss corresponding to both lattice and coordinated water molecules in the range from a bit above room temperature to 116 °C with the experimental mass loss of 16% (calc. mass loss 19.2%). The second stage between 350 and 425 °C attributed to mass loss (calcd/found: 33.0/39.0%) due to decomposition of organic species of the compound. Finally at the temperature range of 500–600 °C a residue is obtained corresponding to the metal oxide, CoO_2 decomposition.

The elemental analysis, spectroscopic studies, thermogravimetric, PXRD results support the structures proposed for **1, 2** and **3** in Fig. 6.

3.5. Vapochromic behavior

4. To test the vapochromic behavior, complex **2a** was activated by heating at 180 °C for 20 min. The complex after activation, was

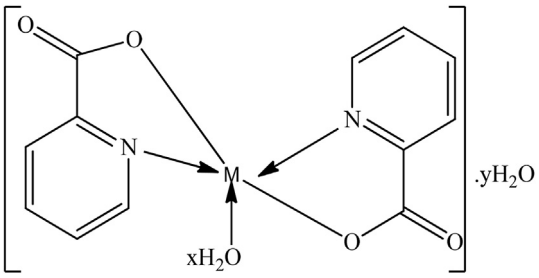


Fig. 6. Proposed structure of synthesized $[M\{Pic\}_2\{H_2O\}_x].yH_2O$, a: obtained through mechanochemical and b: obtained through solvent-based syntheses. Compound **1**: M = Cu, x = 1, y = 0; Compound **2**: M = Co, x = 2, y = 2; Compound **3**: M = Zn, x = 2, y = 2.

named **2d** (Fig. 7). Colour changes were observed after exposing to some solvents, namely ethanol, methanol, dimethyl formamide, dimethyl sulfoxide, benzene, dichloromethane and ammonia for 24 h at room temperature to give **2d**-EtOH, **2d**-MeOH, **2d**-DMF, **2d**-DMSO, **2d**-Benzene, **2d**-DCM and **2d**-NH_3 respectively. The resulting inclusion compounds have different colours depending on the solvent included. The changes in the colour of the complex with VOCs inclusion are given in Fig. 7 and Table S4. Their FT-IR spectra are given in Fig. 8. Solid-state exposure of **2d** to vapours of the above VOCs produces a selective and reversible change in its colour that is perceptible to the human eye and even deeper under UV irradiation, allowing **2d** to function as a sensor for these VOCs. In all the compounds after heating, the O-H band intensity around 3400 cm^{-1} reduces with concomitant water loss, or just a single O-H band is seen. The IR spectra of the activated materials differ from those of the synthesized MOFs.

This indicates structural changes in response to the removal of water molecules. Thus, as a result of heating, the cobalt-aqua bonds were broken and water molecules were lost, resulting in the colour

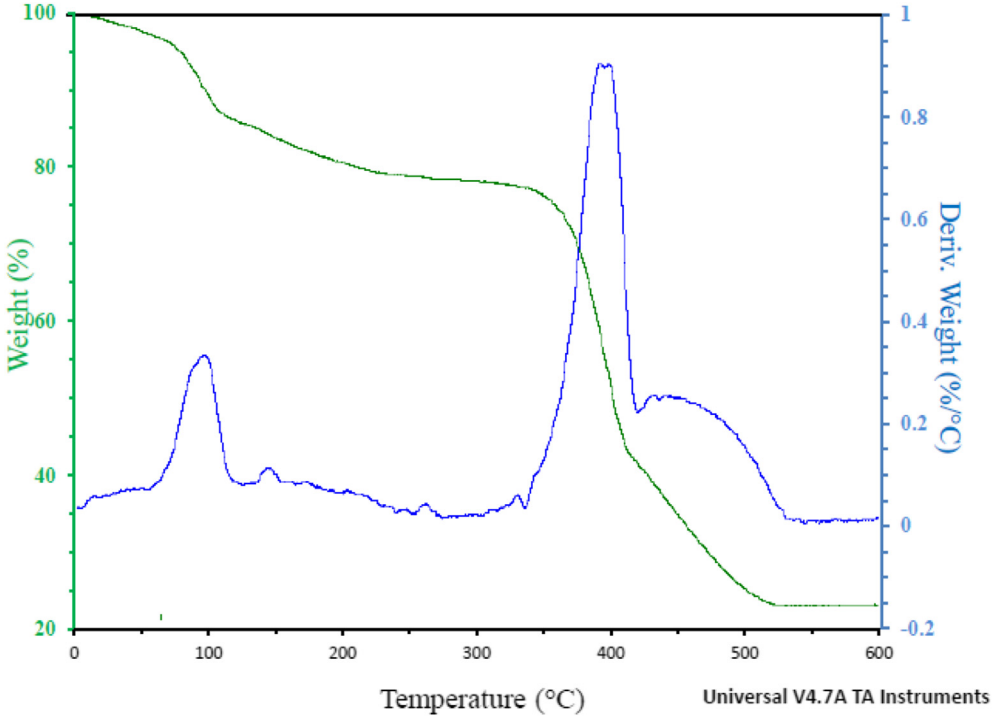


Fig. 5. TGA-DTG curve of **2a**-as synthesized.

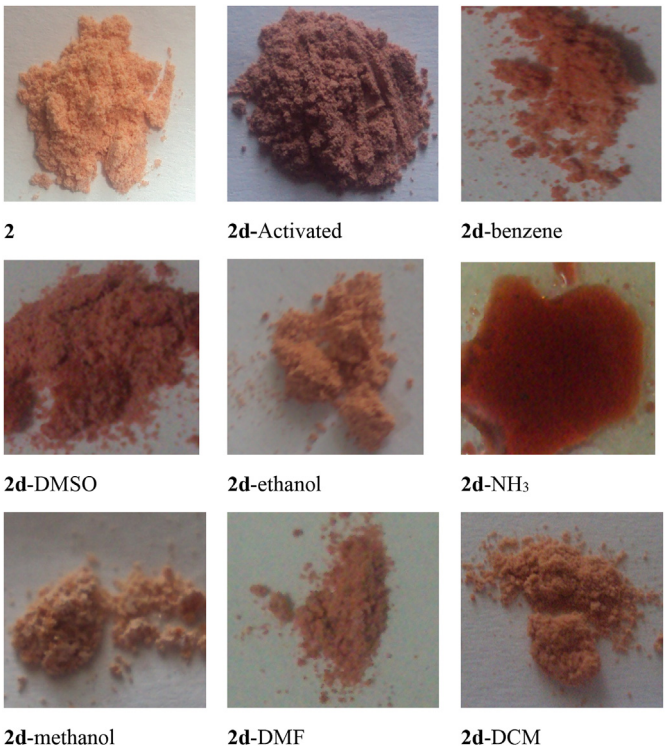


Fig. 7. Pictures of **2a** as-synthesized, after activation and after exposure to VOCs.

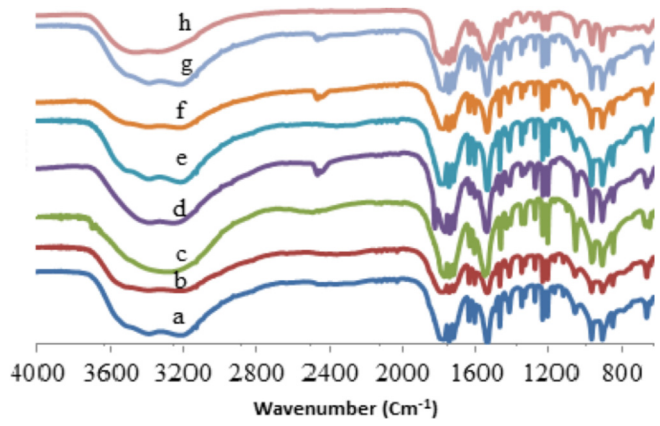


Fig. 8. FT-IR spectra of solvent-included Co-2-Picolinic complexes **2a** (a) **2d**-activated (b) **2d**-Benzene (c) **2d**-DCM (d) 2d-DMF (e) **2d**-DMSO (f) **2d**-ETOH (g) **2d**-MeOH (h) 2d-NH_3.

change. Upon exposure of the activated complexes in ambient environment, water vapour is adsorbed and the colour changed back to the original colours or heating the samples exposed to the VOCs for a few minutes at 100 °C regenerates the original material without degradation, even after several exposure/heating cycles, thus confirming the reversibility of the vapochromic properties.

FTIR study (Fig. 8) shows that peaks were shifted either to lower or higher frequencies for the solvent-included complex as compared to **2d** and appearance of peaks characteristics of functional groups of some of the solvents were observed. The O-H bands observed at 3342 cm^{-1} for **2d** shifted to 3489 cm^{-1}, 3421 cm^{-1}, 3414 cm^{-1}, 3483 cm^{-1}, 3377 cm^{-1} and 3383 cm^{-1} for **2d**-benzene, **2d**-DCM, **2d**-DMF, **2d**-DMSO, **2d**-EtOH and **2d**-MeOH respectively. In **2d**-Benzene the intensity of the aromatic C=C stretch at 1474 cm^{-1} and aromatic C-H stretch at 3147 cm^{-1} increased. There was broad overlapping bands between 3500 and 3200 cm^{-1} attributed to vibration of O-H from coordinated H_2O and N-H. The FTIR results show that, after DMF-included **2d**, an additional peak at 1703 cm^{-1} was found which was not observed after inclusion, using other none carbonyl-derived solvents [41]. The band at 1035 cm^{-1} in **2d**-DMSO can be attributed to the S=O stretching absorption, indicating the presence of DMSO molecules into the complex. Dichloromethane inclusions gave rise to a new peak at 587 cm^{-1} corresponding to (ν C-Cl) stretch. The reaction of ammonia vapour with **2a** is assumed to proceed through liquid phase as revealed by FT-IR and PXRD. FT-IR spectra showed appearance of νN-H band at 3348 cm^{-1} resulting in the formation of complex with formula $[Co(NH_3)(H_2O)_2]^{2+}$. X-ray diffraction pattern of **2a** before and after exposure to ammonia are shown in Fig. S5. Characteristic peaks of **2a** disappear after ammonia adsorption. This indicates that original crystallinity of **2d** was destroyed causing distortion in the morphology of the complex thereby forming liquid. It can be concluded that hydrogen bonding [42] between NH_3 molecule and oxygen atom of the complex caused collapse of the framework of **2a**. This is in agreement with the literature reports [43–46].

Fig. 9 shows the solid state UV-visible spectra of the as-synthesized complex **2**, before and after exposure to volatile organic solvents. The assignments are as shown in Table S5. Comparison of the solid state UV-visible spectra of complex **2d** with those obtained after exposure to VOCs was carried out. The complexes containing the VOCs showed substantial shifts in wavelength and changes in intensity.

The absorption band of the complexes after exposure to VOCs showed blue shift in different solvents to lower wavelength relative to their corresponding complexes. The absorption bands are hypsochromic shifted showing vapochromic response as well as colour change. Complex **2d** showed absorption band at 359 nm after activation and upon direct exposure to VOCs, the absorption band shifted to 339 nm in dimethylformamide, 335 nm in benzene, 345 nm in dichloromethane, 340 nm in acetone and 331 nm in methanol with vapochromic shift λ max in the range 20–28 nm.

Thermogravimetric analysis of the **2d** yielded dehydrated compound (Fig. 10) when compared to the TGA of the synthesized complex **2a** (Fig. 5). The dehydrated 2d complex shows a straight line in the temperature range from room temperature to 350 °C, range in which the organic part of compounds started decomposing. This shows clearly that there were no water molecules in the coordination sphere; complex **2d** was free from water molecules after activation. Again, its decomposition occurred in the same temperature range (350–426 °C) as the organic part of complex **2d**.

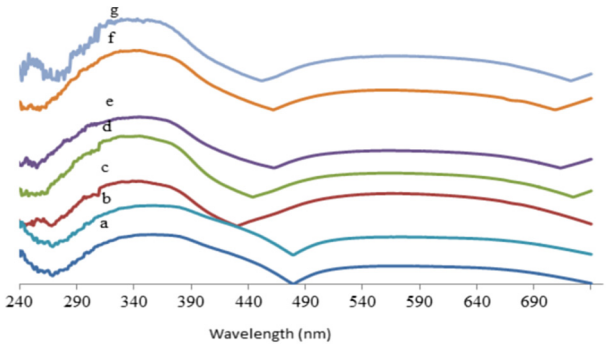


Fig. 9. UV-visible spectra of complex 2, (a) **2a** as-synthesized (b) **2d** (c) **2d**-DMF (d) 2d-Benzene (e) **2d**-DCM (f) **2d**-Acetone and (g) **2d**-Methanol.

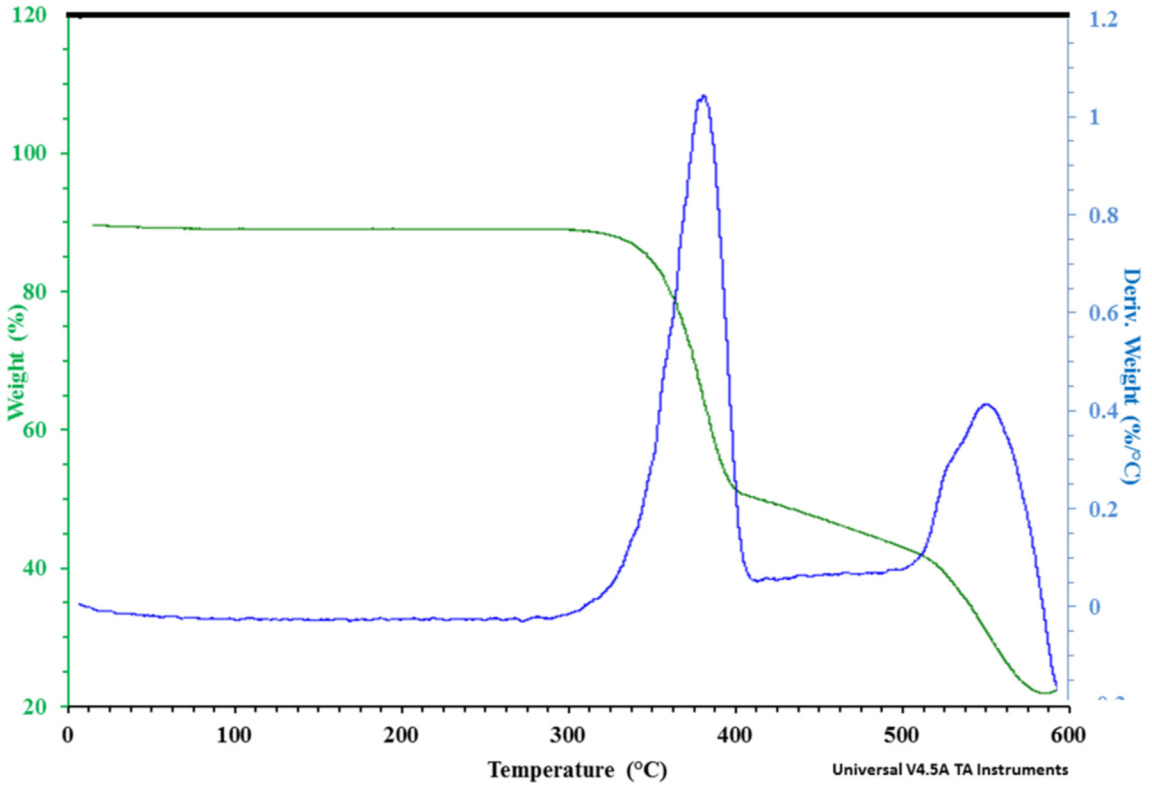


Fig. 10. TGA-DTG curve of complex **2d**.

Table 1
Results of Vapochomic Studies (Host: Guest ratio).

	TGA (%)	Host: Guest ratio
	Experimental data	based on 2d: x
2d – Methanol	14	1: 1.63
2d – Acetone	15	1: 0.97
2d – Benzene	10	1: 0.48
2d – DCM	13	1: 0.57
2d – NH_3	19	1: 4.18

In addition, the sharp peak indicates an endothermic process that eventually ends with the decomposition of the CoO_2 at the temperature range of 530–600 °C.

From the TGA results (Table 1) the sudden weight loss of the **2d**-solvents observed from room temperature to 132 °C were found to be 15%, 14%, 10%, 13% and 19% in **2d**-acetone, **2d**-methanol, **2d**-benzene, **2d**-dichloromethane and **2d**-NH_3 respectively, due to the disappearance of the included solvents. Generally, TGA trace for each of **2d** exposed to solvents also showed plateau in the temperature range of 125–350 °C indicating the high thermal stability of the complex **2** after the absence of the guest molecules. TGA/DTG thermograms depict loss of VOCs with visible endotherms above 100 °C as shown in Fig. 11 and Figs S6–S9. Another clear evidence of reversibility of the reaction is supported by the second endotherms at around 350–425 °C replica endotherm of complex **2d** before exposure to VOCs. The amount of solvents absorbed is given in Table 1. Interestingly the activated phase absorbed ammonia more strongly than other solvents. Absorption of ammonia leads to destruction of the framework as evidenced from loss in crystallinity of the framework. This observation is similar to experimental report that ammonia decomposes frame work [44].

The TGA, FTIR and UV-visible spectra results support absorption of the solvents. Due to the ability of the complex to absorb solvent and the observed change in colour, compound **2** could be employed as solvent-sensor.

Exposure of the complex to VOCs vapours led in some cases, to compounds whose FT-IR spectra clearly show the bands corresponding to the characteristic absorptions of the functional groups of the VOCs employed, perhaps as a consequence of the coordination of the organic molecules to the metal atoms that weakens the bonds. From a structural perspective, it is known that a system does not need to be porous in order to undergo guest uptake [47]. For example, a flexible metal-ligand superstructure can dynamically adapt in order to accommodate a variety of potential guests, as is the case here [47].

Herein, we demonstrate how Co^{2+} ions, well-known for the dramatic colour changes associated with their facile interconversion between octahedral and tetrahedral coordination geometries, can be incorporated into porous solids to produce materials capable of detecting and identifying volatile organic compounds.

4. Conclusion

Metal complexes constructed from Zn(II), Cu(II) and Co(II); and 2-picolinic acid have been synthesized using solvent-free technique and compared with solvent-based methods The mechanochemical method is eco-friendly, simple, efficient and afford excellent yields without solvent or external heating compared to solvent based method. The compounds obtained from both methods were characterized using elemental analysis, PXRD, TGA, FT-IR and UV-Visible spectroscopies. The results showed that, the products of the two methods are identical. Also, vapochromic properties of the Co (II) complexes were studied by exposing it to some volatile organic compounds and ammonia for 24 h after activating the compounds by heating them at 180 °C for 20 min.

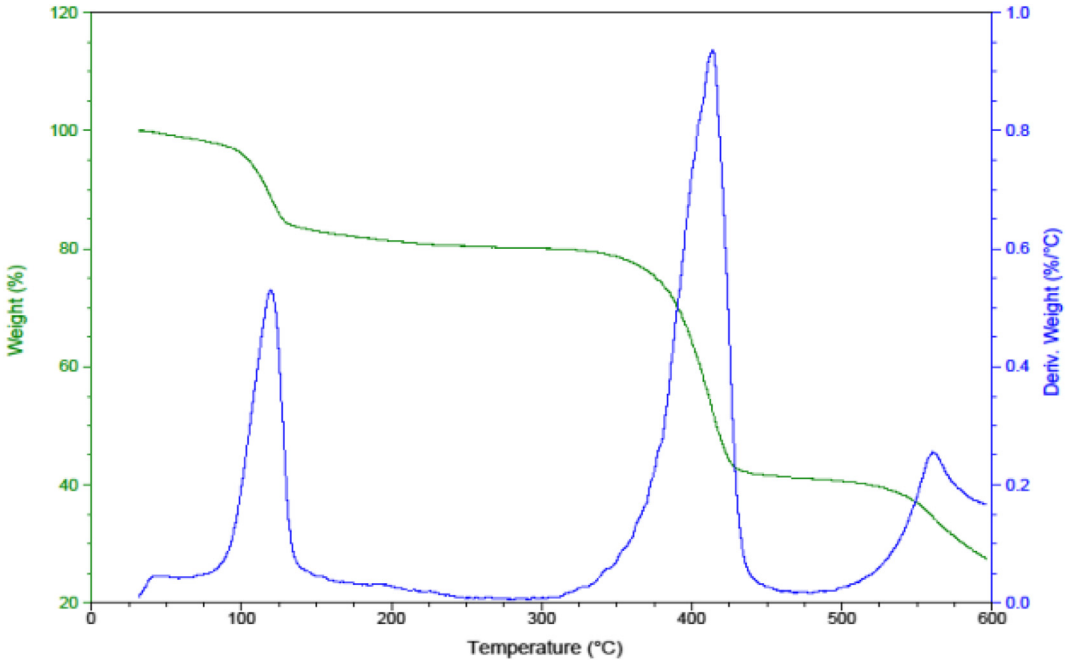


Fig. 11. TGA-DTG curve of solvent-included 2d-acetone.

This resulted into visible colour changes which were monitored by FT-IR and solid state UV-visible spectra and TGA. This inclusion of H-bond donating solvents gave rise to new structural phases whose colours are different from those of the former phases. Host: guest ratio revealed that Co (II) complex 2a has high affinity for ammonia than other solvents, this consequently led to loss in crystallinity and disruption of the framework. These effects are reversible making this complex to display a potential application as sensor for the detection of some solvents.

Acknowledgement

ACT is grateful to the Royal Society of Chemistry for the award of 2013 Research Fund.

Appendix A. Supplementary data

Supplementary data related to this article can be found at http://dx.doi.org/10.1016/j.solidstatesciences.2017.03.017.

References

[1] S. Weenawan, H. Kenneth, J. Cryst. Growth 362 (2013) 252–258.
[2] X. Wang, I. Davis, A. Liu, A. Miller, S.A. Shamsi, J. Chromatogr. A 1316 (2013) 147–153.
[3] S.C. Chuang, A. Fanidi, P.M. Ueland, C. Relton, O. Midttun, S.E. Vollset, M.J. Gunter, M.J. Seckl, R.C. Travis, N. Wareham, et al., Cancer Epidemiol. Biomarkers Prev. 23 (3) (2014) 461–468.
[4] A. Colette, A.M. Ondoh, D.M. Yufanyi, D.S.Y. Gaelle, Int. J. Chem. 7 (1) (2015) 10–20.
[5] G. Sharma, A.K. Narula, J. Mater.Sci. Mater. Electron. 26 (2) (2015) 1009–1017.
[6] D. Li, G. Zhong, Sci. World J. 2014 (2014) 641608.
[7] S. Bahemmat, B. Neumuller, M. Ghassemzadeh, Eur. J. Inorg. Chem. (2015) 4116–4124.
[8] A.C. Tella, S.O. Owalude, L.O. Alimi, A.C. Oladipo, S.J. Olatunji, O.G. Adeyemi, Egypt. J. Basic & Appl. Sci. (EJBAS) 3 (2016) 125–133.
[9] H.A. Salami, A.U. Haruna, F.T. Ezeala, O.W. Salawu, Der Pharma Chem. 7 (4) (2015) 261–265.
[10] A.C. Tella, J.A. Obaleye, U.B. Eke, A.Y. Isaac, O.M. Ameen, Res. Chem. Intermed. 40 (2014) 1441–1457.
[11] A.C. Tella, S.O. Owalude, N. Simon, R.O. Arise, Med. Chem. Res. 24 (2015) 3949–3957.
[12] L. Trobs, M. Wilke, W. Szcerba, U. Reinholz, F. Emmerling, CrystEngComm 16 (2014) 5560–5565.
[13] M. Amin, World J. Pharm. Pharm. Sci. 3 (Issue 4) (2014) 89–99.
[14] C. Tella, U.B. Eke, A.Y. Isaac, A.C. Ojekanmi, Orbit. Electron. J. Chem. 3 (2) (2011) 94–103.
[15] A.C. Tella, S.O. Owalude, J. Mater. Sci. 49 (2014) 5635–5639.
[16] A.C. Tella, O.A. Ameen, P.A. Ajibade, L.O. Alimi, J. Porous Mater 22 (2015) 1599–1605.
[17] A.C. Tella, S.O. Owalude, L.O. Alimi, A.C. Ojekanmi, O.G. Adeyemi, O.S. Olufemi, New J. Chem. 38 (2014) 4494.
[18] G.S. Franziska, E.M. Dreger, E.K. Anorg, Allg. Chem. 639 (5) (2013) 689–693.
[19] J. Lei, R. Qian, P. Ling, L. Cui, H. Ju, Trends Anal. Chem. 58 (2014) 71–78.
[20] A. Pichon, A.L. Garay, S.L. James, CrystEngComm 8 (2006) 211–214.
[21] G. Rottenberg, A.P. Downie, C.L. Raston, J.L. Scott, J. Am. Chem. Soc. 123 (2001) 8701–8703.
[22] A. Munyaneza, M.D. Bala, N.J. Coville, Z. Naturforsch 62b (2007) 453–459.
[23] M.D. Bala, N.J. Coville, J. Organo. Chem. 6932 (2007) 709–773.
[24] F. Drache, V. Bon, I. Senkovska, M. Adam, A. Eychmuller, S. Kaskel, Eur. J. Inorg. Chem. 27 (2016) 4483–4489.
[25] O.B. Pule, S. Degni, N. Torto, Water SA 41 (2015) 27–32.
[26] B. Liu, J. Mater. Chem. 20 (22) (2012) 10094–10101.
[27] C.E. Strasser, V.J. Catalano, J. Am. Chem. Soc. 132 (2010) 10009–10011.
[28] S.H. Lim, M.M. Olmstead, A.L. Balch, J. Am. Chem. Soc. 133 (2011) 10229–10238.
[29] A. Laguna, T. Lasanta, J.M. Lopez-de-Luzuriaga, M. Monge, P. Naumov, M.E. Olmos, J. Am. Chem. Soc. 132 (2010) 456–457.
[30] L.E. Kreno, K. Leong, O.K. Farha, M. Allendorf, R.P. Van Duyne, J.T. Hupp, Chem. Rev. 112 (2012) 1105–1125.
[31] M. Osawa, I. Kawata, S. Igawa, M. Hoshino, T. Fukunaga, D. Hashizume, Chem. Eur. J. 16 (2010) 12114–12126.
[32] G. Li, L. Li, J. Liu, T. Yang, C. Su, Cryst. Growth & Des. 13 (4) (2013) 1518–1525.
[33] P.P. Silva, W. Guerra, J.N. Silveira, A.M. Ferreira, T. Bortolotto, F.L. Fischer, H. Terenzi, A. Neves, E.C.P. Maia, Inorg. Chem. 50 (2011) 6414–6424.
[34] C. Jobbagy, T. Tunyogi, G. Palinkas, A. Deak, Inorg. Chem. 50 (2011) 7301–7308.
[35] M.O. Agwara, N.B. Ndosiri, A. Mohamadou, A.M. Condé, Res. J. Pharm. Biol. Chem. Sci. 4 (2) (2013) 1370–1381.
[36] B.-M. Kukovec, M. Kaksa, Z. Popovic, Croat. Chem. Acta. 85 (2012) 479–483.
[37] B. Zurowska, J. Ochocki, J. Mrozinski, Z. Ciunik, J. Reedijk, Inorg. Chim. Acta. 357 (3) (2004) 755–763.
[38] Z.K. Jacimovic, M. Kosovic, S.B. Novakovic, G. Giester, A. Radovic, J. Serb. Chem. Soc. 80 (7) (2015) 867–875.
[39] A.C. Tella, S.O. Owalude, P.A. Ajibade, N. Simon, S.J. Olatunji, M.S.M. Abdelbaky, S. Garcia-Granda, J. Mol. Struct. 1125 (2016) 570–575.
[40] Z. Heren, C.C. Ersanli, C. Keser, N.O. Ocak İskeleli, Acta Cryst. E62 (4) (2006) 796–798.
[41] B. Fang, T. Wang, X. Chen, T. Jin, R. Zhang, W. ZhuanG, J. Phys. Chem. B 119 (38) (2015) 12390–12396.

[42] D. Saha, S. Deng, J. Colloid Interface Sci. 348 (2) (2010) 615–620.
[43] M.J. Katz, A.J. Hawartt, Dalton Trans. 45 (2016) 4150.
[44] G.W. Peterson, G.W. Wagner, A. Balboa, J. Mahle, T. Sewell, C.J. Karwacki, J.Phys Chem. C Nanomater. Interfaces 113 (31) (2009) 13906–13917.
[45] C. Petit, T.J. Bandosz, Adv. Funct. Mater. 20 (2010) 111–118.
[46] E. Barea, C. Montoro, J.A.R. Navarro, Chem. Soc. Rev. 43 (2014) 5419.
[47] J. Lefebvre, J.L. Korčok, M.J. Katz, D.B. Leznoff, Sensors (Basel) 12 (3) (2012) 3669–3692.